Dielectronic satellite spectra of hydrogenlike iron from the Tokamak Fusion Test Reactor

V. Decaux
Laboratoire de Physique Atomique et Nucléaire, Institut du Radium, Université Pierre et Marie Curie, 75005 Paris, France

M. Bitter, H. Hsuan, S. von Goeler, K. W. Hill, R. A. Hulse, G. Taylor, and H. Park
Plasma Physics Laboratory, Princeton University, Princeton, New Jersey 08544

C. P. Bhalla
Department of Physics, Kansas State University, Manhattan, Kansas 66506
(Received 28 June 1990)

Spectra of hydrogenlike iron Fe XXVI have been observed from Tokamak Fusion Test Reactor plasmas with a high-resolution crystal spectrometer. The experimental arrangement permits simultaneous observation of the Fe XXVI Ly-α_1 and Ly-α_2 lines and the associated dielectronic satellites, which are due to transitions $1snl$-$2pnl'$ with $n \geq 2$, as well as the heliumlike $1s^2(^1S_0)$-$1s4p(^1P_1)$ and both hydrogenlike Ly-β_1 and Ly-β_2 lines from chromium. Relative wavelengths and line intensities can be determined very accurately. The spectral data are in very good agreement with theoretical calculations. The observed spectra have also been used to estimate the total dielectronic recombination rate coefficient of Fe XXVI.

I. INTRODUCTION

Spectra of hydrogenlike iron Fe XXVI have been previously observed from solar flares[1,2] and beam-foil experiments.[3] The main interest in data from solar flares resides in their potential application to plasma diagnostics, especially a determination of the electron temperature from the relative intensities of the Ly-α lines and their associated dielectronic satellites. On the other hand, the goal of the beam-foil experiments has been to perform very accurate absolute wavelength measurements of the Ly-α_1 and Ly-α_2 lines in order to determine the $1s$ Lamb shift and to test predictions of quantum electrodynamics (QED) for higher-Z ions. The wavelengths measured by Briand *et al.*[3] were in very good agreement with calculations from Erickson[4] and Mohr.[5,6] These beam-foil experiments, however, did not show satellites of the Ly-α lines. In fact, special care was taken to avoid contamination of the Ly-α_1 and Ly-α_2 lines from high-n satellites by an appropriate choice of the target foil thickness.

The satellites of the Ly-α lines are of purely dielectronic nature, in contrast to the well-documented case of heliumlike ions,[7–12] where the satellites of the resonance line can also originate from collisional inner-shell excitation. The satellite spectra of hydrogenlike ions are therefore important for an understanding of the process of dielectronic recombination. Unfortunately, due to low count rates[1] or insufficient spectral resolution,[2] the data obtained so far from solar flares have not permitted a detailed comparison of the dielectronic satellites' features of Fe XXVI with theory.

Spectra of Fe XXVI can also be recorded from large tokamak plasmas, e.g., Joint European Torus (JET) and Tokamak Fusion Test Reactor (TFTR), which contain metal impurities in small concentrations (typically 0.1% of the electron density n_e). In these tokamaks, plasmas with central electron densities $n_3(0) \leq 10^{20}\ m^{-3}$ and central electron temperatures $T_e(0) \approx 5$ keV can be maintained under steady-state conditions for several seconds. Under these conditions, the ion charge state distribution of the metal impurities approaches the coronal equilibrium. However, deviations from coronal equilibrium can occur as a result of radial ion transport. The line-excitation mechanisms for high-Z ions in these plasmas are similar to those in solar flares, due to the fact that the electron densities are well below the critical value for collisional deexcitation. Since the plasma conditions are reproducible, spectra can be recorded with small statistical errors. Since n_e and T_e are determined from independent diagnostics, it is possible to make a detailed comparison of these spectra with theory.

In this paper, we discuss Fe XXVI spectra which have been obtained from TFTR plasmas with a high-resolution crystal spectrometer. We also present spectra of chromium lines, i.e., the heliumlike $1s^2(^1S_0)$-$1s4p(^1P_1)$ transition and the hydrogenlike Ly-β_1 and Ly-β_2 lines, which were observed simultaneously with the Fe XXVI spectra. This makes it possible to determine the wavelengths for these transitions relative to the Fe XXVI Ly-α lines and to verify the theoretically predicted Z dependence. The experimental data are compared with results from the multiconfiguration Dirac-Fock model (MCDF), Hartree-Fock-Slater[13] (HFS) calculations, as well as the theoretical predictions of Erickson,[4] Vainshtein and Safronova,[14] and Dubau *et al.*[15] Also estimated from HFS calculations are the contributions from the satellites to the chromium resonance lines, especially the satellites of the $1s^2(^1S_0)$-$1s4p(^1P_1)$ transition. These calculations em-

ploy the Hartree-Fock-Slater atomic model to obtain the single-particle wave functions.[16,17]

II. EXPERIMENTAL RESULTS

Figure 1 shows the experimental arrangement and a schematic of the TFTR vertical spectrometer used for these measurements. The spectrometer consists of five arms which record x-ray line spectra from impurity ions at different vertical sight lines with major radii $R=2.41$, 2.55, 2.63, 2.89, and 2.96 m. Instrumental details have been described in Ref. 18. The spectra of hydrogenlike iron are recorded by the arm with a near-central sight line at $R=2.63$ m, while the other four arms record spectra from heliumlike iron. The Fe XXVI spectra were measured with a bent ($20\bar{2}3$; $2d=2.7497$ Å) quartz crystal of $6\times1.5\times0.030$ in.[3] and a position-sensitive multiwire proportional counter in the Johann configuration.[19] The radius of curvature of the crystal was 12.268 m and the spectral resolution was $\lambda/\Delta\lambda\approx10\,000$ Å at $\lambda=1.7780$ Å. The Johann configuration permitted simultaneous observation of spectral lines in the wavelength range from 1.760 to 1.805 Å.

Figure 2 presents the observed spectrum. It shows the satellite spectrum of Fe XXVI and, in addition, features of Cr XXIII and Cr XXIV. The data were accumulated from 14 nearly identical TFTR discharges with a central electron density $n_e(0)\approx1.4\times10^{19}$ m^{-3} and a central electron temperature $T_e(0)\approx5$ keV during a 2-s period of steady-state conditions. The radial profiles of the electron density and electron temperature were measured with a far-infrared interferometer and an electron cyclotron emission radiometer, respectively, and are shown in Fig. 3. The spectrum presented in Fig. 2 shows a relatively high

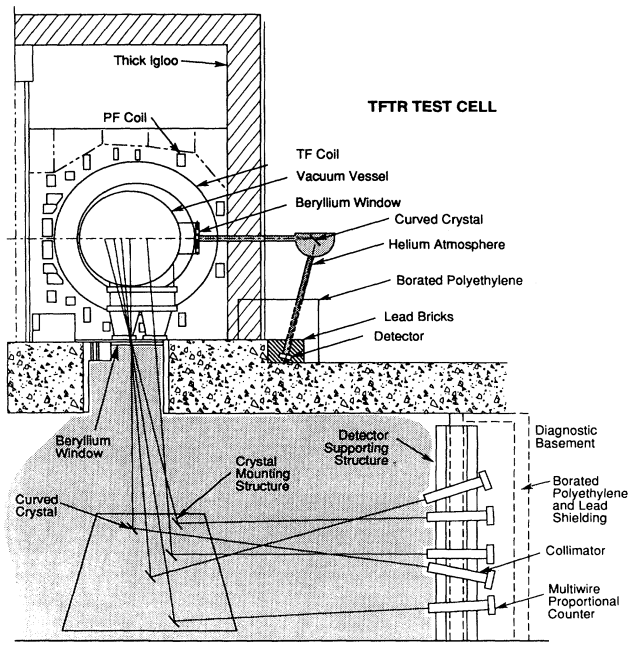

FIG. 1. Experimental arrangement.

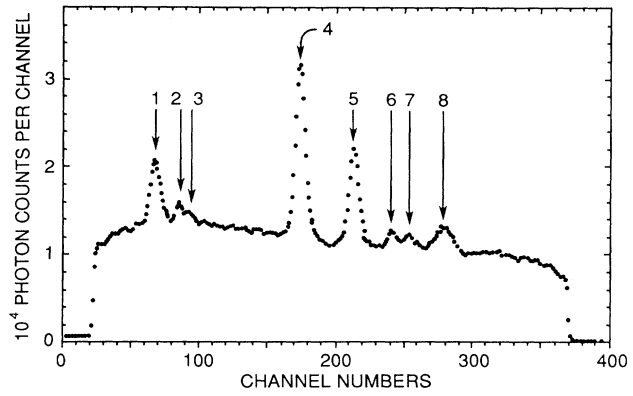

FIG. 2. Observed x-ray spectrum. The spectrum consists of the Fe XXVI Ly-α lines with the associated dielectronic satellites, the Cr XXIII $1s^2(^1S_0)$-$1s4p(^1P_1)$ transition, and the Cr XXIV Ly-β lines.

background of continuum radiation from bremsstrahlung and recombination. This is due to the fact that the heliumlike Fe XXV is the dominant charge state, and that the fractional abundance $n_{\text{Fe XXVI}}/n_{\text{Fe XXV}}$ was only 0.12.

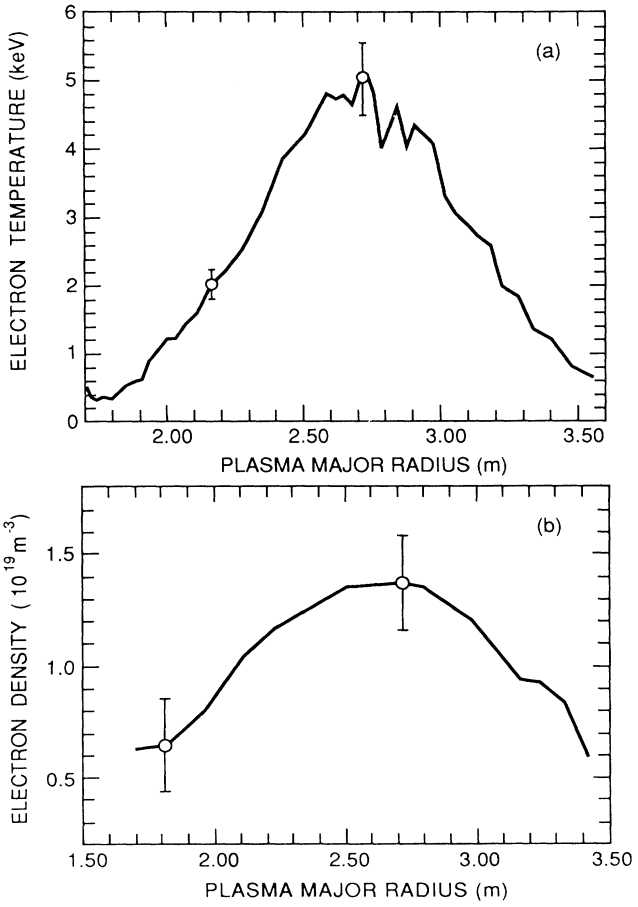

FIG. 3. Radial profiles of (a) the electron temperature measured from the electron cyclotron emission radiometer and (b) the electron density obtained from the TFTR far-infrared interferometer.

TABLE I. Experimental wavelengths and theoretical predictions for the resonance lines of chromium and iron. Wavelengths are given in angstroms and the peaks refer to Fig. 2. Asterisks denote chromium features; the other peaks are iron features.

Peak	Transition	N	λ_{expt}	λ_{theor} [b] (MCDF)	λ_{theor} [c]	λ_{theor} [e]
1	$1s^2(^1S_0)$-$1s4p(^1P_1)$*	67.55	1.763 3	1.763 67	1.7634[d]	
2	$1s(^2S_{1/2})$-$3p(^2P_{3/2})$*	85.32	1.765 8	1.765 70	1.7659	1.765 717(6)
3	$1s(^1S_{1/2})$-$3p(^2P_{1/2})$*	92.31	1.766 8	1.766 84	1.766 8	1.766 862(6)
4	$1s(^2S_{1/2})$-$2p(^2P_{3/2})$	173.86	1.778 04[a]		1.7780	1.778 04(1)[a]
5	$1s(^2S_{1/2})$-$2p(^2P_{1/2})$	212.97	1.783 4		1.7834	1.783 46(1)

[a]The experimental wavelengths are normalized to the theoretical values of the Fe XXVI $1s(^2S_{1/2})$-$2p(^2P_{3/2})$ transition.
[b]Present calculations with a multiconfiguration Dirac-Fock (MCDF) program and QED corrections.
[c]Reference 14.
[d]This wavelength was calculated as explained in the text.
[e]Reference 4; the values in parentheses represent the uncertainty on the last digit inferred from the QED uncertainties.

This value of $n_{\text{Fe XXVI}}/n_{\text{Fe XXV}}$ was inferred from a comparison of the measured intensities of the Fe XXVI Ly-α lines with the Fe XXV $1s^2(^1S_0)$-$1s2p(^1P_1)$ resonance line, recorded at $R=2.55$ m. For comparison $n_{\text{Fe XXVI}}/n_{\text{Fe XXV}}=0.4$ for coronal equilibrium. From calculations of the ionization equilibrium with a one-dimensional multiion species transport (MIST) code,[20] which takes into account cross field ion transport, in addition to processes of ionization and recombination, we found that the observed ratio of 0.12 is consistent with a radial diffusion coefficient of $2\times10^4\text{cm}^2\,\text{s}^{-1}$.

Tables I and II list experimental wavelengths, as well as results of our calculations which are based on the MCDF code of Grant, McKenzie, and Norrington,[21] for the chromium and iron features shown in Fig. 2. The code includes corrections arising from the finite nuclear size, the vacuum polarization, and the self-energy. The QED corrections are usually considered as a sum of the last two corrections. Features 1–3 have been identified as the $1s^2(^1S_0)$-$1s4p(^1P_1)$ transition of Cr XXIII, and the Ly-$\beta_{1,2}$ lines of Cr XXIV. Features 4 and 5 are the Fe XXVI Ly-α lines, and features 6–8 are the associated

TABLE II. Experimental wavelengths and predictions from different theoretical models, MCDF, HFS, TF, and Z expansion, for the main $n=2$ satellites of Fe XXVI shown in Fig. 2. Wavelengths are given in angstroms and satellite line strengths $F_2^*(s)$ are in units of $10^{13}\,\text{s}^{-1}$.

Peak	Key	Transition	N	λ_{expt}	λ_{theor} [a] (MCDF)	λ_{theor}	$F_2^*(s)$
6	T	$1s2s(^1S_0)$-$2s2p(^1P_1)$	241.15	1.7873	1.787 096	1.7865[b]	16.19[b]
						1.7861[c]	−7[e]
						1.7871[d]	4[f]
	K	$1s2p(^3P_2)$-$2p^2(^1D_2)$			1.787 117	1.7871[b]	10.26[b]
						1.7870[c]	−11[e]
						1.7873[d]	4[f]
7	Q	$1s2s(^3S_1)$-$2s2p(^3P_2)$	253.62	1.7890	1.788 109	1.7882[b]	3.27[b]
						1.7881[c]	−1[e]
						1.7881[d]	−1[f]
	B	$1s2p(^3P_1)$-$2p^3(^2P_2)$			1.788 760	1.7887[b]	7.22[b]
						1.7882[c]	−10[e]
						1.7888[d]	9[f]
8	J	$1s2p(^1P_1)$-$2p^2(^1D_2)$	278.98	1.7924	1.792 08	1.7919[b]	32.96[b]
						1.7917[c]	−5[e]
						1.7970[d]	0[f]
	A	$1s2p(^3P_2)$-$2p^2(^3P_2)$			1.792 54	1.7925[b]	12.19[b]
						1.7921[c]	−8[e]
						1.7925[d]	4[f]

[a]New calculations performed with a multiconfiguration Dirac-Fock (MCDF) code.
[b]Reference 13; Hartree-Fock-Slater (HFS) calculations.
[c]Reference 15; scaled Thomas-Fermi (TF) model.
[d]Reference 14; Z-expansion technique.
[e]Reference 15; percentage differences $=100[x(\text{TF})-x(\text{HFS})]/x(\text{HFS})$.
[f]Reference 14; percentage difference $=100[x(Z\text{ expansion})-x(\text{HFS})]/x(\text{HFS})$.

most prominent $n=2$ satellites. The listed theoretical wavelength of 1.7634 Å for the $1s^2(^1S_0)$-$1s4p(^1P_1)$ transition of Cr XXIII was obtained by adding the energies of the Cr XXIII $1s4p(^1P_1)$-$1s2s(^1S_0)$ and $1s2s(^1S_0)$-$1s^2(^1S_0)$ transitions given by Vainshtein and Safronova.[14] The same value was found from an estimate by Wiese and Musgrove,[22] using the difference of calculated binding energies for the $n=4$ level from Ermolaev and Jones[23] and the binding energy of the ground state from Safronova.[24] The listed channel numbers N correspond to the center positions of the observed spectral features. They were determined from a least-mean-squares fit of Voigt functions to the experimental data. The experimental wavelengths were then evaluated from Eq (1):

$$\lambda = 2d \sin(\theta_0 + \Delta\theta) , \quad (1)$$

where $\Delta\theta(\text{deg}) = 3.753 \times 10^{-3}(N - N_0)$ is given by the dispersion of the instrument. N_0 is the center channel of the Ly-α_1 line (feature 4). Since the spectrometer has no absolute wavelength calibration, the Ly-α_1 line was taken as a reference, normalizing $\lambda_0 = 2d \sin\theta_0$ to the theoretical value $\lambda_0 = 1.778\,04$ Å from Erickson.[4] For comparison, the value given by Johnson and Soff,[25] who performed the most accurate calculations for hydrogenlike ions, is $\lambda_0 = 1.778\,016\,3(1)$ Å. The experimental error for the wavelength measurements is ±0.2 mÅ. The key letters of the $1s2l$-$2p2l'$ dielectronic satellites of Fe XXVI in Table II correspond to Safronova's notation. The experimental wavelengths have been compared with MCDF and HFS (Ref. 13) calculations. They are also compared with the theoretical results of Dubau *et al.* from the scaled Thomas-Fermi (TF) model[15] and the predictions of Vainshtein and Safronova, who used the Z-expansion technique.[14] We note that both the TF and HFS results include an overall 0.8-mÅ shift to account approximately for the QED corrections. Also listed are the satellite line strengths, $F_2^*(s) = F_2(s)/\omega_g$, obtained from the HFS calculations, which are compared with values given by Dubau *et al.*[15] and Vainshtein and Safronova.[14] ω_g represents the statistical factor of the ground state. For the present case, $\omega_g = 2$. We note that the $F_2(s)$ values for the strong satellite lines from Ref. 14 are in much better agreement (within 4%) with the corresponding values from the HFS calculations, while the results of Ref. 15 are consistently lower by ≈10%.

In order to make a detailed comparison of the observed Fe XXVI dielectronic satellite spectrum with theory, it is necessary to first consider the possible contamination of this spectrum by satellites of the Cr XXIII $1s^2$-$1s4p$ transition and of the Cr XXIV Ly-β lines, which fall into the wavelength range from 1.780 to 1.800 Å. For this purpose, we calculated the wavelengths and the line strengths $F_2^*(s)$ of the $1s^22l$-$1s2l'4p$ satellites using the HFS model. The results are listed in Table III. [Note

TABLE III. Theoretical data for the main $n=2$ satellites of the Cr XXIII $1s^2(^1S_0)$-$1s4p(^1P_1)$ transition. Wavelengths are in angstroms, satellite line strengths $F_2^*(s)$ are in units of 10^{13} s^{-1}, energies E_S are in keV, and relative satellite to resonance line intensities I_S/I_R are in percent.

Transition	λ_{theor}	$F_2^*(s)$	E_S	I_S/I_R
$1s2s(^1S)4p(^2P_{3/2})$-$1s^22s(^2S_{1/2})$	1.7806	1.145	5.241	3.52
$1s2s(^1S)4p(^2P_{1/2})$-$1s^22s(^2S_{1/2})$	1.7808	0.447	5.240	1.38
$1s2p(^3P)4s(^2P_{1/2})$-$1s^22s(^2S_{1/2})$	1.7812	0.049	5.238	0.16
$1s2p(^3P)4s(^4P_{1/2})$-$1s^22s(^2S_{1/2})$	1.7825	0.012	5.233	0.04
$1s2p(^1P)4p(^2D_{3/2})$-$1s^22p(^2P_{1/2})$	1.7848	0.017	5.268	0.06
$1s2p(^1P)4p(^2P_{3/2})$-$1s^22p(^2P_{3/2})$	1.7873	0.039	5.270	0.12
$1s2s(^3S)4p(^2P_{1/2})$-$1s^22s(^2S_{1/2})$	1.7874	0.365	5.214	1.12
$1s2s(^3S)4p(^2P_{3/2})$-$1s^22s(^2S_{1/2})$	1.7875	0.737	5.214	2.26
$1s2p(^1P)4p(^2D_{5/2})$-$1s^22p(^2P_{3/2})$	1.7875	0.153	5.269	0.46
$1s2p(^1P)4p(^2D_{3/2})$-$1s^22p(^2P_{3/2})$	1.7877	0.086	5.268	0.26
$1s2s(^3S)4p(^4P_{3/2})$-$1s^22s(^2S_{1/2})$	1.7881	0.084	5.211	0.26
$1s2p(^3P)4p(^2S_{1/2})$-$1s^22p(^2P_{1/2})$	1.7881	0.033	5.256	0.10
$1s2p(^3P)4p(^2P_{3/2})$-$1s^22p(^2P_{1/2})$	1.7890	0.016	5.252	0.04
$1s2p(^3P)4p(^2S_{3/2})$-$1s^22p(^2P_{3/2})$	1.7910	0.386	5.256	1.18
$1s2p(^3P)4p(^2D_{3/2})$-$1s^22p(^2P_{1/2})$	1.7913	1.486	5.243	4.56
$1s2p(^3P)4p(^2D_{5/2})$-$1s^22p(^2P_{3/2})$	1.7914	5.498	5.254	16.86
$1s2p(^3P)4p(^2P_{1/2})$-$1s^22p(^2P_{1/2})$	1.7914	0.094	5.243	0.28
$1s2p(^3P)4p(^2P_{3/2})$-$1s^22p(^2P_{3/2})$	1.7919	0.658	5.252	2.02
$1s2p(^3P)4p(^4S_{3/2})$-$1s^22p(^2P_{1/2})$	1.7922	0.134	5.240	0.42
$1s2p(^3P)4p(^2P_{5/2})$-$1s^22p(^2P_{3/2})$	1.7923	0.716	5.251	2.20
$1s2p(^3P)4p(^4P_{3/2})$-$1s^22p(^2P_{3/2})$	1.7923	0.253	5.251	0.78
$1s2p(^1S)4p(^2S_{1/2})$-$1s^22p(^2P_{1/2})$	1.7937	0.020	5.234	0.06
$1s2p(^3P)4p(^4D_{5/2})$-$1s^22p(^2P_{3/2})$	1.7948	0.038	5.241	0.12
$1s2p(^3P)4p(^4S_{3/2})$-$1s^22p(^2P_{3/2})$	1.7951	0.024	5.240	0.08
$1s2s(^3S)4d(^2D_{3/2})$-$1s^22p(^2P_{1/2})$	1.7978	0.061	5.218	0.18
$1s2s(^3S)4s(^2S_{1/2})$-$1s^22p(^2P_{1/2})$	1.8002	0.049	5.209	0.16
$1s2s(^3S)4d(^2D_{5/2})$-$1s^22p(^2P_{3/2})$	1.8007	0.056	5.218	0.18
$1s2s(^3S)4s(^2S_{1/2})$-$1s^22p(^2P_{3/2})$	1.8031	0.051	5.209	0.16

that the wavelength value for the $1s^2(^1S_0)$-$1s4p(^1P_1)$ resonance line obtained from these HFS calculations is 1.7617 Å, without any adjustment.] The relative intensities of the satellites and the resonance line (Table III) are given by Eq. (2):

$$\frac{I_S}{I_R}=F_1(T_e)F_2(s)\ , \tag{2}$$

where

$$F_1(T_e)=\frac{5.24\times10^{-27}T_e^{-3/2}e^{-E_S/kT_e}}{C_R(T_e)}\ , \tag{3}$$

$$F_2(s)=\omega_s\frac{A_a^{sg}A_r^{sf}}{\sum_{g'}A_a^{sg'}+\sum_{f'}A_r^{sf'}}=\omega_g F_2^*(s)\ . \tag{4}$$

A_a^{sg} is the autoionization rate from the state $|s\rangle$ and the ground state $|g\rangle$; the sum over g' extends over all the states of the (Z) ion accessible by autoionization from the state $|s\rangle$. A_r^{sf} is the radiative transition from the state $|s\rangle$ to the state $|f\rangle$; the sum over f' relates to all the lower states of the $Z-1$ ion. ω_S is the statistical weight of the upper level. T_e is the electron temperature in keV, and E_S are the energy differences between the $1s2l4p$ level of lithiumlike Cr XXII and the ground state of heliumlike Cr XXIII listed in Table III. $C_R(T_e)\approx1.08\times10^{-13}$ cm^3 s^{-1} at $T_e=5$ keV is the excitation rate coefficient for the resonance line given by Sampson, Goett, and Clark.[26] The I_S/I_R values calculated for this electron temperature are listed in Table III. Most of these satellites are very weak. Therefore they do not perturb the iron spectrum. A possible exception is the $1s2p(^3P)4p(^2D_{5/2})$-$1s^22p(^2P_{3/2})$ satellite, the intensity of which is about 15% of the $1s^2(^1S_0)$-$1s4p(^1P_1)$ resonance line, and which may be blended with the line *J*.

The satellites of the Cr XXIV Ly-β lines are in the wavelength range from 1.765 to 1.800 Å.[27] The contribution of these satellites to the spectrum is negligible, since the intensity of the Ly-β lines is very small.

In the following, we compare the observed dielectronic satellite spectrum of Fe XXVI with synthetic spectra. The synthetic spectra were constructed from the theoretical data for the Ly-α lines and the main $n\leq3$ satellites of the HFS calculations[13] and Refs. 15 and 14, respectively. For this purpose, we first calculated radial emissivity profiles for each spectral line using the iron charge state distribution obtained from the MIST code calculations and the measured electron density and electron temperature profiles. The line intensities were then evaluated from chord integrals of these emissivity profiles. The obtained synthetic spectra are presented in Fig. 4. For the wavelengths of the Ly-α resonance lines in Figs. 4(b) and 4(c) we took the values of Erickson.[4] The synthetic spectra are in good general agreement with the experimental data. The wavelengths given by the HFS calculations and by Vainshtein and Safronova are in better agreement with the experiment than those of Dubau *et al.*

It is also of interest to estimate the total dielectronic recombination rate coefficient α_d for Fe XXVI, since this

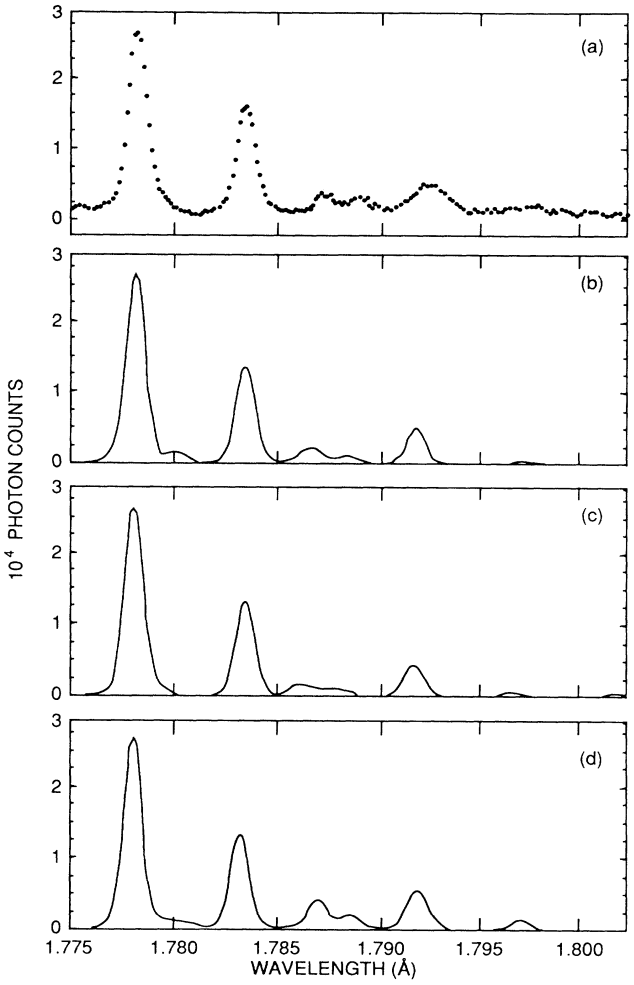

FIG. 4. Fe XXVI spectra: (a) observed spectrum after background correction, (b), (c), and (d) synthetic spectra constructed from theoretical data from Hartree-Fock-Slater calculations (Ref. 13) and Refs. 15 and 14, respectively.

coefficient is of importance for transport code calculations of the ion charge state distribution. For this purpose, we use the expression

$$\alpha_d=C_R(T_e)\sum_S\frac{I_S}{I_R}\ , \tag{5}$$

where $\sum_S I_S/I_R$ is the sum of the *observed* dielectronic satellite intensities relative to the intensity of the resonance lines, and $C_R(T_e)$ is the collision excitation rate coefficient for the resonance transitions *taken from theory*. Expression (5) is a good approximation if the line radiation is emitted from a region with a nearly constant electron temperature. For our experimental conditions, the main contribution to the observed spectra originates from a near-central region ($R=2.63\pm0.20$ m) of the plasma, due to the fact that the excitation energies for the Ly-α lines and the associated satellites are 6.9 eV and 5.2

keV, respectively. However, contributions from noncentral regions are not negligible. In fact, our calculations of the emissivity profiles indicate that the noncentral contributions are 35% for the Ly-α lines and 45% for the $n=2$ satellites. Equation (5) can therefore only be used for a rough estimate.

Evaluating from Fig. 4(a) the experimentally observed satellite structure between $\lambda=1.785-1.800$ Å, and taking for I_R the intensity between $\lambda=1.775$ and 1.785 Å, we obtain for $\sum_S I_S/I_R$ a value of 0.42, and a value of 0.34 after subtracting the contribution from the chromium $1s^2 2l$-$1s 2l' 4p$ satellites (Table III). We have not made any corrections for the contribution of the $n \geq 3$ satellites to the Ly-α resonance lines, since this contribution is small for the experimental electron temperatures. The largest uncertainty results from the value for $C_R(T_e)$. Using for $C_R(T_e)$ the expression from Vainshtein, Safronova, and Urnov,[28]

$$C_R(T_e)=10^{-8}\left[\frac{E_\alpha}{E_{\alpha_0}}\frac{E_H}{E_{\alpha\alpha_0}}\right]^{3/2}(B_{1/2}+B_{3/2})\left[\frac{E_{\alpha\alpha_0}}{T_e}\right]^{1/2}\exp\left[-\frac{E_{\alpha\alpha_0}}{T_e}\right]\frac{E_{\alpha\alpha_0}/T_e+\delta_{S_1S_2}}{E_{\alpha\alpha_0}/T_e+\chi}\ , \tag{6}$$

where $E_\alpha=169$ Ry, $E_{\alpha_0}=676$ Ry, $E_H=1$ Ry, $E_{\alpha\alpha_0}=507$ Ry, $B_{1/2}=11.3$, $B_{3/2}=22.7$, $\chi=0.24$, and $\delta_{S_1S_2}=1$, and inserting for T_e the peak electron temperature of 5 keV, we obtain an *upper bound* value $\alpha_d=5.3\times10^{-13}$ cm^3 s^{-1}. For comparison, the theoretical predictions for this electron temperature of Dubau *et al.*[15] and Burgess[29] are 3×10^{-13} cm^3 s^{-1} and 3.8×10^{-13} cm^3 s^{-1}, respectively. Note that the calculations of $C_R(T_e)$ from Dubau *et al.* and Burgess show a wide maximum between 3 and 7 keV. The value of Dubau *et al.* could be obtained from Eq. (5) if we assumed a value of $T_e=3.4$ keV in the calculation of $C_R(T_e)$. Since the experimentally observed data represent line-averaged intensities from a region with variable electron temperature, it is more realistic to use an averaged value of the electron temperature rather than the peak value of 5 keV. An averaged value of $T_e=3.4$ keV is not inconsistent with our experiment.

III. CONCLUSION

The simultaneous observation of features from both chromium and iron made it possible to verify the Z dependence of the wavelength calculations. We find that the present MCDF and the Z-expansion calculations with QED corrections are in very good agreement with the experimental data. An overall 0.8-mÅ wavelength shift from nonrelativistic calculations, as suggested in Ref. 15, is almost sufficient to account for higher-order effects. We note that the satellite line intensity factors for the strong satellite lines from the HFS (Ref. 13) calculations are in excellent agreement (within 4%) with the results from the Z-expansion technique[14] and in a reasonable agreement ($\leq 10\%$) with the TF (Ref. 15) results.

Synthetic spectra constructed from the predictions of the HFS (Ref. 13) and the TF (Ref. 15) models as well as the Z-expansion technique[14] are in good general agreement with the observed spectra.

The experimental data have also been used to estimate the dielectronic recombination rate coefficient of Fe XXVI. A value of $\alpha_d=3\times10^{13}$ cm^3 s^{-1} is obtained for an average electron temperature of 3.4 keV, which is in agreement with the theoretical predictions.[15,29,30]

ACKNOWLEDGMENTS

We gratefully acknowledge the support of Dr. H. P. Furth, Dr. P. Rutherford, Dr. D. M. Meade, Dr. K. M. Young, and the technical assistance of J. Gorman and R. Such, and the TFTR operating crew. We also thank Dr. J. P. Briand for fruitful discussions. This work was supported by the U.S. Department of Energy (DOE), Contract No. DE-AC02-76-CHO-3073. One of us (C.P.B.) was supported by the Division of Chemical Sciences, Office of Basic Energy Sciences, Office of Energy Research, U.S. DOE.

[1]A. N. Parmar, J. L. Culhane, C. G. Rapley, E. Antonucci, A. H. Gabriel, and M. Loulergue, Mon. Not. R. Astron. Soc. **197**, 29 (1981).

[2]F. Moriyama, K. Tanaka, K. Akita, T. Watanabe, H. Miyazaki, H. Miyashita, K. Kumagai, and K. Nishi, Ann. Tokyo Astron. Obs. **19**, 276 (1983).

[3]J. P. Briand, M. Tavernier, P. Indelicato, R. Marrus, and H. Gould, Phys. Rev. Lett. **59**, 832 (1983).

[4]G. W. Erickson, J. Phys. Chem. Ref. Data **6**, 831 (1977).

[5]P. J. Mohr, Phys. Rev. Lett. **34**, 1050 (1975).

[6]P. J. Mohr, Ann. Phys. (N.Y.) **88**, 26 (1974); **88**, 52 (1974).

[7]Y. I. Grineva, V. I. Karov, V. V. Korneev, V. V. Krutov, S. L. Mandelstam, L. A. Vainshtein, B. N. Vasilysev, and J. A. Zhitnik, Sol. Phys. **29**, 441 (1973).

[8]A. H. Gabriel, J. L. Culhane, L. W. Acton, E. Antonucci, R. D. Bentley, C. Jordan, L. W. Leibacher, A. N. Parmar, K. J. H. Phillips, C. G. Rapley, C. J. Wolfson, and K. T. Strong, Adv. Space Res. **1**, 267 (1981).

[9]M. Bitter, K. W. Hill, N. R. Sauthoff, P. C. Efthimion, E. Meservey, W. Roney, S. von Goeler, R. Horton, M. Goldman, and W. Stodiek, Phys. Rev. Lett. **43**, 129 (1979).

[10]M. Bitter, S. von Goeler, K. W. Hill, R. Horton, D. Johnson, W. Roney, N. Sauthoff, E. Silver, and W. Stodiek, Phys. Rev. Lett. **47**, 921 (1981).

[11]T. F. R. Group, J. Dubau, and M. Loulergue, J. Phys. B **15**, 1007 (1982).

[12]F. Bely-Dubau, P. Faucher, L. Steenman-Clark, M. Bitter, S. von Goeler, K. W. Hill, C. Camhy-Val, and J. Dubau, Phys. Rev. A **26**, 3459 (1982).
[13]C. P. Bhalla and K. R. Karim, Rev. Sci. Instrum. **59**, 1527 (1988).
[14]L. A. Vainshtein and U. I. Safronova, Academy of Science of the U.S.S.R., P. N. Lebedev Institute of Spectroscopy, Report No. 2, 1985 (unpublished).
[15]J. Dubau, A. H. Gabriel, M. Loulergue, L. Steenman-Clark, and S. Volonté, Mon. Not. R. Astron. Soc. **195**, 705 (1981).
[16]C. P. Bhalla and K. R. Karim, Phys. Rev. A **34**, 3525 (1986).
[17]K. R. Karim and C. P. Bhalla, Phys. Rev. A **34**, 4743 (1986).
[18]M. Bitter, K. W. Hill, S. Cohen, S. von Goeler, H. Hsuan, L. C. Johnson, S. Raftopoulos, M. Reale, N. Schechtman, S. Sesnic, F. Spinos, J. Timberlake, S. Weicher, N. Young, and K. M. Young, Rev. Sci. Instrum. **57**, 2145 (1986).
[19]H. Johann, Z. Phys. **69**, 189 (1931).
[20]R. A. Hulse, Nucl. Technol. Fusion **3**, 259 (1983).
[21]I. P. Grant, B. J. McKenzie, and P. H. Norrington, Comput. Phys. Commun. **21**, 207 (1980); **21**, 233 (1980).
[22]W. L. Wiese and A. Musgrove, Oak Ridge National Laboratory Report No. ORNL-6551/V2, 1989.
[23]A. M. Ermolaev and M. Jones, J. Phys. B **7**, 199 (1974).
[24]U. I. Safronova, Phys. Scr. **23**, 241 (1981).
[25]W. R. Johnson and G. Soff, At. Data Nucl. Data Tables **33**, 405 (1985).
[26]D. H. Sampson, S. J. Goett, and R. E. H. Clark, At. Data Nucl. Data Tables **29**, 467 (1983).
[27]L. A. Vainshtein and U. I. Safronova, At. Data Nucl. Data Tables **25**, 311 (1980).
[28]U. I. Safronova, A. M. Urnov, and L. A. Vainshtein, Proc. P. N. Lebedev, Phys. Int. [Acad. Sci. USSR **119**, 13 (1980)].
[29]A. Burgess, Astrophys. J. **141**, 1588 (1965).
[30]K. R. Karim and C. P. Bhalla, Phys. Rev. A **37**, 2599 (1988).